Title
New withanolides with TRAIL-sensitizing effect from Physalis pubescens L.

Journal
RSC Advances, 6(58)

ISSN
2046-2069

Authors
Chen, Li-Xia
Xia, Gui-Yang
He, Hao
et al.

Publication Date
2016

DOI
10.1039/c6ra07031k

Peer reviewed

Published in final edited form as:

RSC Adv. 2016 ; 6(58): 52925–52936. doi:10.1039/C6RA07031K.

New withanolides with TRAIL-sensitizing effect from *Physalis pubescens* L.

Li-Xia Chen[a,b], **Gui-Yang Xia**[a,c], **Hao He**[d], **Jian Huang**[a], **Feng Qiu**[a,c,*], and **Xiao-Lin Zi**[b,*]

[a]Department of Natural Products Chemistry, School of Traditional Chinese Materia Medica, Key Laboratory of Structure-Based Drug Design & Discovery, Ministry of Education, Shenyang Pharmaceutical University, Shenyang 110016, People's Republic of China

[b]Department of Urology, University of California, Irvine, Orange, CA 92868, USA

[c]School of Chinese Materia Medica and Tianjin State Key Laboratory of Modern Chinese Medicine, Tianjin University of Traditional Chinese Medicine, Tianjin 300193, People's Republic of China

[d]School of Pharmaceutical Sciences, Xi' an Medical University, Xi' an 710021, People's Republic of China

Abstract

Physalis pubescens L. plant produces nutritious and healthy fruits, called husk tomato or hairy ground cherry. However, its bioactive components are largely unknown. Four new withanolide steroids (**1–4**) together with one known withanolide (**5**) were isolated from the extract of *P. pubescens* L. and their chemical structures were established by extensive spectroscopic analyses. Compounds **1**, **3** and **5** showed potent growth inhibitory effects against four human renal cell carcinoma (RCC) cell lines (i.e. 786-O, A-498, Caki-2 and ACHN). Among them, compound **1** was the most potent one with IC_{50}s ranged from 0.30 to 0.77 μM. Further experiment showed that **1** sensitized human RCC cells 786-O to the tumor necrosis factor related apoptosis ligand (TRAIL)-induced apoptosis and increased the expression of C/EBP-homologous protein (CHOP) and death receptor-5 (DR5), leading to activation of the DR5 and caspase-8/3 mediated apoptosis pathway. Molecular docking analysis revealed that compound **1** could bind stably to the TRAIL/DR5 complex through hydrogen bonds. These results suggest that the new withanolide (**1**) is a lead anti-cancer compound existing in *P. pubescens* L. and deserves further investigation for RCC prevention and treatment.

Graphical Abstract

fengqiu20070118@163.com; Tel.: +86-22-59596223. xzi@uci.edu; Tel.: +01-714-456-8316.

†Electronic supplementary information (ESI) available: HRESIMS, IR, UV, 1D NMR, and 2D NMR spectra, as well as HPLC and UPLC-QTOF-MS chromatograms for new withanolides **1–4**. See DOI:

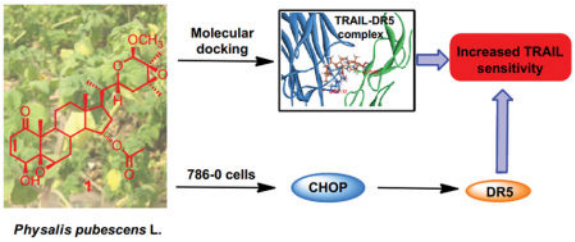

Introduction

The incidence of kidney cancer is continuously rising and becomes the ninth most common cancer in the world. Renal cell carcinoma (RCC) accounts for about 90% of adult kidney cancers.[1,2] Surgical resection provides curative treatment for most RCCs, but approximately 30% of patients eventually develop recurrence and metastasis. The five-year survival rates of metastatic RCCs are below 10%. Treatment for metastatic RCC has recently been transformed due to introduction of molecularly targeted agents, such as tyrosine-kinase inhibitors, mammalian target of rapamycin (mTOR) inhibitors and Bevacizumab. Although these agents have been proved to increase the overall survival of RCC patients, their therapeutic effects are short-live and development of drug resistance is almost inevitable for every treated RCC patient. Therefore, new agents for the treatment of metastatic RCC are still urgently needed.

TRAIL is a member of the tumor necrosis factor (TNF) superfamily that induces apoptosis through recognizing and binding to its cognate receptors on cell surfaces, namely TRAIL receptor 1 (DR4) and TRAIL receptor 2 (DR5). Upon binding to DR4 or DR5, TRAIL initiates the trimerization of receptors to form the death-inducing signaling complex, which in turn activates caspase-8 and -10 mediated apoptosis.[3,4] TRAIL represents an attractive therapeutic target due to its selective killing of a variety of tumor cells, yet relatively nontoxic to normal cells.[5] However, many cancer cells have been shown to be resistant to apoptotic effects induced by TRAIL.[6,7] Therefore, agents that can sensitize cancer cells to the apoptotic effects of TRAIL are highly desirable to be developed as new cancer therapeutic agents.

Natural products are rich resources for identifying TRAIL-sensitizing agents for cancer therapy and prevention.[8–10] However, the biological potencies of previously identified TRAIL-sensitizers are still not completely satisfied because their effective concentrations are within micromolar range. Withanolides are a group of naturally occurring C_{28} steroids derived from an ergostane skeleton and usually functionalized at C-1, C-22 and C-26.[11,12] This type of steroid has attracted significant attention due to their diverse structures and multiple bioactivities such as cytotoxic,[13,14] anti-inflammatory[15,16] and immunoregulatory[17,18] activities, *etc.*. The genus *Physalis* (Solanaceae), a rich source of withanolides, includes about 120 species throughout tropical and subtropical regions of the world.[19] The fruits of *Physalis pubescens* L. (Chinese name: Deng-Long-Cao and English name: husk tomato or hairy ground cherry), a kind of nutritious and healthy berries, have been used as a traditional folk medicine in China for the treatment of sore throat, cough and

urogenital system diseases such as urethritis, hematuria and orchitis.[20] Although some withanolides have been identified from this plant,[21,22] its bioactive components are still largely unknown.

We have previously found that the crude extract of *P. pubescens* L. possessed *in vitro* growth inhibitory effects against four human RCC cell lines (786-O, A-498, Caki-2 and ACHN) with IC_{50} values of 334.2, 350.9, 329.6 and 549.7 μg/mL, respectively. As part of our ongoing research for biologically active withanolides from the genus *Physalis*,[12,16] a phytochemical investigation on the fruits of *P. pubescens* L. was carried out for finding potentially more potent TRAIL-sensitizers as a new treatment in RCC. Four new withanolide steroids (**1–4**) together with one known withanolide (**5**) (Figure 1) were isolated from this plant and their chemical structures were characterized by spectroscopic methods. The new withanolide (**1**) from *P. pubescens* L. is a lead compound that can reduce the viabilities of four human RCC cell lines (786-O, A-498, Caki-2 and ACHN) at nanomolar concentrations by induction of apoptosis and acts as a potent TRAIL-sensitizer. The mechanism of the new withanolide (**1**) inducing apoptosis may be involved in CHOP mediated up-regulation of DR5 expression and its direct binding to the TRAIL/DR5 complex.

Results and discussion

The known withanolide (**5**), an inseparable epimeric mixture, was identified as (20*S*,22*R*, 24*R*,25*S*,26*S*)-15α-acetoxy-5,6β:22,26-diepoxy-4β,24,25,26- tetrahydroxyergost-2-en-1-one (**5a**) and (20*S*,22*R*,24*R*,25*S*,26*R*)-15α-acetoxy-5,6β:22,26-diepoxy-4β,24,25,26-tetrahydroxyergost-2-en-1-one (**5b**) by comparing their NMR spectroscopic data with those of the published values.[23]

The molecular formula for **1** was defined as $C_{31}H_{44}O_8$ by HRESIMS (*m/z* 567.2925 $[M+Na]^+$, calcd. for 567.2928). The IR spectrum of **1** showed absorptions for hydroxyl (3397 cm^{-1}), ester (1734 cm^{-1}) and α,β-unsaturated ketone (1663 cm^{-1}) groups. The NMR spectroscopic data (Tables 1 and 2) of **1** suggested that it possessed the typical withanolide skeleton. The presence of a 5β,6β-epoxy-4β-hydroxy-2-en-1-one unit in rings A and B was deduced by analyzing the ^{1}H NMR spectrum [$\delta_{H\text{-}2}$ 6.16 (1H, d, J = 10.0 Hz), $\delta_{H\text{-}3}$ 6.90 (1H, dd, J = 10.0, 5.8 Hz), $\delta_{H\text{-}4}$ 3.72 (1H, d, J = 5.8 Hz), $\delta_{H\text{-}6}$ 3.19 (1H, br s)] and the ^{13}C NMR spectrum [$\delta_{C\text{-}1}$ 202.3, $\delta_{C\text{-}2}$ 132.1, $\delta_{C\text{-}3}$ 142.1, $\delta_{C\text{-}4}$ 69.8, $\delta_{C\text{-}5}$ 63.6, $\delta_{C\text{-}6}$ 62.6]. The HMBC correlations from CH_3-19 to C-1, C-5, C-9 and C-10 further confirmed the above substitution pattern. The NMR data of **1** closely resembled those of physapubescin[23] except for the nine-carbon side chain, especially the chemical shift of C-26. One additional methoxy signal compared to physapubescin was observed in both ^{1}H NMR [δ_H 3.37 (3H, s)] and ^{13}C NMR (δ_C 55.7) spectra of **1**. In the HMBC spectrum, the methoxy signal at δ_H 3.37 correlated with the hemiacetal carbon at δ_C 99.3 (C-26), and the hemiacetal proton at δ_H 4.58 (H-26) correlated with the methoxy carbon at δ_C 55.7, indicating that the methoxyl should be located at C-26. The 20*S*, 22*R* configurations of **1** were determined based on the biogenetic considerations and the characteristic small coupling pattern (3.6 Hz) of two *gauche* conformation protons, H-20 and H-22 (Figure 2).[24,25] The characteristic NOESY correlations of H_3-21/H-23$_{ax}$, H-17/H-23$_{eq}$, H_2-16/H-22 and H-22/H-20 further confirmed

the 20*S*, 22*R* configurations.[25] The NOESY experiment showed cross-correlations of H-26/H_3-27, H-23_{ax}/H_3-28 and H-22/H-23_{eq}, whereas no correlations of H-22/H_3-27 and H-22/H_3-28, suggesting H-26, CH_3-27 and CH_3-28 were *trans* to H-22. Taking all above data and biosynthetic grounds into consideration, the structure of **1** was assigned as (20*S*, 22*R*,24*S*,25*S*,26*R*)-15α-acetoxy-5,6β:22,26:24,25-triepoxy-26-methoxy-4β-hydroxyergost-2-en-1-one.

The ESI-MS of compound **2** showed two quasi-molecular ions $[M+Na]^+$ at *m/z* 589 and $[M+2+Na]^+$ at *m/z* 591 with the ratio of 3:1, which indicated the presence of one chlorine atom. And this was confirmed by the HRESIMS which showed a quasi-molecular ion $[M+Na]^+$ at *m/z* 589.2532 analyzing for $C_{30}H_{43}O_8ClNa^+$ (calcd. for 589.2539), consistent with the molecular formula $C_{30}H_{43}O_8Cl$. In the IR spectrum of **2**, absorption bands at 3461, 1735 and 1683 cm^{-1} suggested the presence of hydroxyl, ester and α,β-unsaturated ketone groups, respectively. The ^1H NMR (Table 1) spectrum showed characteristic methyl signals at δ_H 0.69 (3H, s), 0.82 (3H, d, J = 6.6 Hz), 1.23 (3H, s), 1.37 (3H, s), 1.38 (3H, s) and 2.03 (3H, s), and two olefinic signals at δ_H 6.00 (1H, d, J = 10.2 Hz) and 6.47 (1H, d, J = 10.2 Hz). The ^{13}C NMR (Table 2) and HSQC spectra revealed 30 carbons and the almost identical ^{13}C NMR data for rings C–D and the side chain to those of physapubescin, the first withanolide isolated from this plant,[26] indicating that their structural differences were restricted to substituents in rings A and B. The strong up-field shift of the carbon resonance of CH_3-19 (from δ_C 17.7 in physapubescin to δ_C 9.9 in **2**) is typical of a 5β-hydroxy-6α-chloro arrangement.[26] An α-orientation of the chlorine atom was determined by the spin-spin coupling pattern of H-6 at δ_H 4.37 (1H, dd, J = 11.8, 4.3 Hz).[27] The characteristic coupling pattern of H-22 and the NOESY correlations suggested 20*S*, 22*R* configurations.[24,25] According to the above data and biosynthetic grounds, the structure of **2** was elucidated as (20*S*,22*R*,24*S*,25*S*,26*R*)-15α-acetoxy-6α-chloro-22,26:24,25-diepoxy-4β,5β,26-trihydroxyergost-2-en-1-one.

Compound **3** was isolated as an inseparable epimeric mixture (**3a** and **3b**) as shown during HPLC analysis (Figure S27), and their ratio was determined as 1.5:1 from the relative integration areas of the respective resonances of H-26 at δ_H 5.25 and 5.36. The molecular formulas of **3a**/**3b** were determined to be $C_{31}H_{46}O_9$ on the basis of HRESIMS. Comparison of the ^{13}C NMR data of **3** (Table 2) with those of **5**[23] revealed the down-field shift of C-24 and the presence of a new methoxyl in **3a**/**3b**. The HMBC correlations between -OCH_3 (δ_H 3.55/3.56) and C-24 (δ_C 77.6/78.6) suggested that **3a**/**3b** should be the methyl ether derivatives of **5**. The 20*S*, 22*R* configurations of **3a**/**3b** were determined through the characteristic coupling pattern of the C-22 hydrogen: δ_H 3.73 (1H, dt, J = 12.4, 2.9 Hz)/4.41 (1H, dt, J = 12.4, 2.8 Hz), and NOE correlations of H_3-21/H-23_{ax}, H-17/H-23_{eq}, H-16α/H-22, H-16β/H-22 and H-22/H-20.[19, 25] The 24*R*, 25*S* configurations were correspondingly determined by the NOESY correlations of H_3-28/H-22 and H_3-27/OCH_3-24. On the basis of the above findings and biosynthetic considerations, the major (**3a**) and minor (**3b**) stereoisomers were determined as (20*S*,22*R*,24*R*,25*S*,26*S*)-15α-acetoxy-5,6β:22,26:diepoxy-24-methoxy-4β,25,26- trihydroxyergost-2-en-1-one and (20*S*,22*R*,24*R*,25*S*,26*R*)-15α-acetoxy-5,6β:22,26:diepoxy-24-methoxy-4β,25,26-trihydroxyergost-2-en-1-one, respectively.

Compound **4** was also isolated as an unresolvable epimeric isomer as shown during HPLC analysis (Figure S35). The ratio of two epimers (**4a** and **4b**) was determined as 1.9:1 according to the relative integration areas of the respective resonances of H-26 at δ_H 5.39 and 5.52. Their molecular formulas $C_{30}H_{46}O_{10}$ were deduced by HRESIMS, which displays eight degrees of unsaturation. The IR spectrum showed the presence of hydroxyl (3433 cm^{-1}) and saturated-δ-lactone (1712 cm^{-1}) groups. The ^{13}C NMR chemical shift values (Table 2) pertaining to rings C–D and the side chain in **4a**/**4b** were identical to those of **5**,[23] while the difference was observed only in ring A. The appearance of two signals at δ_C 44.4 and 69.6 in **4a**/**4b** and the disappearance of two olefinic carbons in **5** suggested that **4a**/**4b** are a derivative of **5** bearing a hydroxyl group at C-3.[28] This deduction was supported by the HMBC correlations from H-2 to C-1/C-3/C-4/C-10, H-3 to C-1/C-4/C-5, and H-4 to C-2/C-3/C-4/C-10. NOE correlations of CH_3-19 with H-2β, as well as H-2α with H-3 and H-4 suggested that both of H-3 and H-4 were α-oriented. The 20*S*, 22*R* configurations of **4a**/**4b** were also determined based on the biogenetic considerations and the characteristic small coupling pattern (2.5 Hz) of two *gauche* conformation protons, H-20 and H-22.[24,25] And the characteristic NOESY correlations of H_3-21/H-23_{ax}, H-17/H-23_{eq}, H-16α/H-22, H-16β/H-22 and H-22/H-20 further confirmed the 20*S*, 22*R* configurations.[25] NOESY correlation of H-22/H_3-28, but no correlation of H-22/H_3-27 suggested the stereo configurations of C-24 and C-25 to be *R* and *S*, respectively. On the basis of the above evidences and biosynthetic grounds, the structures of the major (**4a**) and minor (**4b**) stereoisomers were identified as (20*S*,22*R*,24*R*,25*S*,26*S*)-15α-acetoxy-5,6β:22,26-diepoxy-3β,4β,24,25,26- pentahydroxyergost-1-one and (20*S*,22*R*,24*R*,25*S*,26*R*)-15α-acetoxy-5,6β:22,26- diepoxy-3β,4β,24,25,26-pentahydroxyergost-1-one, respectively.

We have attempted to purify the interconverting epimers of **3**–**5** through crystallization from mixed solvents (MeOH–H_2O and CH_2Cl_2–MeOH) according to the method reported in literature.[29] Unfortunately, we also couldn't obtain the pure major diastereomer due to the pure form was rapidly epimerized to 26*S* and 26*R* mixtures.

The growth inhibitory effects of compounds **1**–**5** were tested against four human RCC cell lines (786-O, A-498, Caki-2 and ACHN) and measured by MTT method.[30] Cells were cultured with 0, 0.15625, 0.3125, 0.625, 1.25, 2.5, 5 and 10 μM compounds **1**–**5** for 72 hours (h). The results showed that **1**, **3** and **5** reduced cell viabilities in a dose-dependent manner (Figure 3A). The data revealed that the functional groups of a 4β-hydroxy-2-en-1-one in ring A and a 5β,6β-epoxy in ring B are important for the activities of withanolides. In particular, **1** showed the most potent growth inhibitory effects against the four human RCC cell lines with IC_{50} values in the range of 0.30–0.77 μM. Compound **2** with partial absence of the functional groups aforementioned showed no growth inhibitory effects against these cell lines at the same concentrations (Data not shown). These results are in agreement with previous structure-activity relationship reports.[12] We are currently unable to discuss the structure-activity relationship of the inseparable epimeric mixtures (**3**–**5**), owing to the difference in the ratio of two epimers in each mixture. Since **1** is the most potent one among the identified withanolides from this plant and 786-O cells are most sensitive to the cytotoxic effects of **1**, **1** and 786-O were therefore prioritized for investigating its underlying mechanism of action in the following experiments.

In order to ascertain the cytotoxicity of **1** in normal human cells, human embryonic kidney cells (HEK 293) were treated with 0, 1.25, 2.5, 5, and 10 μM of compound **1** for 48 and 72 h. Also, the cells were treated with the same doses of 5-fluorouracil (5-Fu) as positive control. The results showed that the cell viability of HEK 293 treated with **1** was better than when treated with 5-Fu (Figure 3B), indicating that the toxicity of **1** is lower than the clinical anticancer drug 5-Fu. Taken together, **1** exhibited no significant cytotoxicity towards normal human cells, exhibiting good selectivity.

Compound **1** inhibited 786-O cell growth in a dose-dependent manner with an IC_{50} value (at 72 h) of 0.30±0.07 μM (Figure 3A). To determine whether the growth inhibitory effect of compound **1** against 786-O cells is through the induction of apoptosis, the morphological changes of control- and **1**-treated cells were observed under light and fluorescence microscopes. Compared to vehicle control, treatment of 786-O cells with **1** caused typical apoptotic morphological changes, including cell shrinkage and rounding up, cell membrane blebbing, as well as nuclear fragmentation and condensation (Figures 4A and 4B). In addition, flow cytometric analysis showed a significant increase in both early (Annexin V staining only, right-lower panels) and late apoptosis (Annexin V and PI staining, right-upper panels) populations as compared to control treatment, with 41.7±4% apoptotic cells in **1**-treated 786-O cells, vs. 4.5±0.3% in control (Figure 4C). Together, these results suggested that **1** induces apoptotic cell death in 786-O cells.

It is well known that apoptosis can be induced by the extrinsic pathway associated with death receptor stimulation on the cell surface,[31] and by the intrinsic pathway involved in mitochondrial dysfunction, leading to activate caspase-8 and caspase-9 mediated apoptosis pathways, respectively.[10] To investigate whether **1** activates caspase cascade along the apoptotic pathway, caspase-3 and caspase-8 were detected by Western blot analysis. A dose-dependent cleavage of procaspase-3 and procaspase-8, as well as poly-ADP-ribosepolymerase (PARP) was observed in **1**-treated cells (Figure 5A). In addition, caspase activation was determined with caspase-3/7 and caspase-8 activity assays. Figure 5B showed a dose-dependent increase of caspase-3 and -8 activities by about 16~176% in **1**-treated 786-O cells compared to those treated by vehicle control.

To determine whether **1**-induced apoptosis is related to the intrinsic mitochondria pathway, the integrity of mitochondrial membranes of 786-O cells was examined by rhodamin 123 staining. As shown in Figure 6A and 6B, 1 treatment did not almost decrease the fluorescence intensity, indicating **1** could not significantly induce mitochondrial depolarization in 786-O cells. Also, the expression of Bcl-2, Bax, and caspase-9 proteins previously reported to be important for intrinsic apoptosis signaling,[32,33] which was almost not affected by **1** treatment (Figure 6C). These above results suggested that **1** may activate the death-receptor mediated apoptotic pathway leading to activation of caspase-8/3 cascade, but not a caspase-9-dependent intrinsic pathway.

To further investigate the effects of **1** on the death-receptor mediated apoptosis, Western blot analysis was carried out, showing that compound **1** markedly increased the protein expression of DR5 and CHOP in a dose-dependent manner (Figure 7A). CHOP is a major transcriptional factor for up-regulating the expression of DR5.[34] Additionally, 786-O cells

treated with 2 μM compound **1** and 100 ng/mL TRAIL alone reduced cell viabilities by 52 and 9%, respectively, while the combined treatment with both agents led to a significant decrease of cell viability to 83% (Figure 7B). Similarly, Annexin V staining showed that treatment with either 1 μM compound **1** or 100 ng/mL TRAIL alone resulted in about 18 or 17% of 786-O cells undergoing apoptosis, whereas combination of both agents increased the ratio of apoptotic cells to 43% (Figure 7C). Taken together, these observations suggested that **1** potentiates the apoptotic effect of TRAIL ligand via induction of CHOP-mediated up-regulation of DR5 expression.

Using the CDOCKER protocol, molecular docking analysis identified a potential binding conformation of compound **1** in the TRAIL/DR5 complex. After molecular docking, the ligand structure with the most favorable binding free energies and reasonable orientations was selected as the optimal docked conformation. As shown in Figure 8, compound **1** stably binds to interface of the TRAIL/DR5 complex. Two hydrogen bonds, ARG-132 of TRAIL and ARG-115 of DR5 were formed, which played an important role in the ligand–protein interactions. Thus, compound **1** may also directly interact with the TRAIL/DR5 complex to sensitize the apoptotic effect of TRAIL.

In this study, we showed for the first time that the new withanolide (**1**) from *P. pubescens* L. induced apoptosis on human RCC cells 786-O via activation of the extrinsic death receptor-mediated apoptotic pathway. Our results further suggested that **1** effectively sensitized human RCC cells 786-O to TRAIL-induced apoptosis through up-regulation of CHOP-mediated DR5 expression and direct binding to the TRAIL/DR5 complex. Up to date, only two literatures reported that withanolides, withanolide E[35] from *P. peruviana* and withaferin A[36] from *Withania somnifera* showed TRAIL-sensitizing effects in human RCC cells, ACHN and Caki-2, respectively, with a mechanism of c-FLIP degradation. The discovery of a new and potent withanolide from *P. pubescens* L. as a TRAIL sensitizer in our study is consistent with these two previous literatures. However, it is also reported that small structural differences might lead to significant diversity in activity, for example, the C2, C3 double bond in ring A and a 5β,6β-epoxy in ring B can enhance cytotoxicity,[37–40] and the C4 hydroxyl increases toxicity in many cell types, but has little effect on sensitization of ACHN cells to TRAIL.[35] The chemical structures of withanolides isolated from *P. pubescens* L. in this study are obviously different from withanolide E and withaferin A with a new nine-carbon side chain, which may contribute to the observed difference in their biological activities. Therefore, further experiments are in progress to examine whether the epoxy-δ-lactol and α,β- unsaturated δ-lactone side chains will affect the differential sensitizing effects of withanolides to TRAIL-induced apoptosis.

Conclusions

In summary, four previously unreported withanolide steroids (**1–4**) together with one known withanolide (**5**) were isolated from *P. pubescens* L.. Compounds **1**, **3** and **5** showed potent growth inhibitory effects against four human renal cell carcinoma (RCC) cell lines (786-O, A-498, Caki-2 and ACHN). Among them, the newly identified withanolide (**1**) is a lead TRAIL-sensitizing compound from *P. pubescens* L. and could potentially be developed for treatment of cancer with resistance to TRAIL-based therapies. However, in order to fully

realize the potential of compound **1** as a new therapeutic or preventative agent for RCC, further studies are still needed to elucidate its mechanism of action and anti-tumor activities *in vivo* in animal models, as well as its pharmacokinetic and pharmacodynamics characteristics.

Experimental section

General experimental procedures

Optical rotations were measured with a PerkinElmer 241 polarimeter. UV spectra were recorded on a Shimadzu UV 2201 spectrophotometer, and IR (4000–400 cm^{-1}) spectra (KBr pellets) were recorded on a Bruker IFS 55 spectrometer. NMR experiments were performed on Bruker ARX-300 and AV-600 spectrometers. Chemical shifts are stated relative to TMS and expressed in δ values (ppm), with coupling constants reported in Hz. HRESIMS were obtained on an Agilent 6210 TOF mass spectrometer. Silica gel GF254 prepared for TLC and silica gel (200–300 mesh) for column chromatography (CC) were obtained from Qingdao Marine Chemical Factory (Qingdao, People's Republic of China). Sephadex LH-20 was a product of Pharmacia (Uppsala, Sweden). Octadecyl silica gel (ODS) was purchased from Merck Chemical Company Ltd. RP-HPLC separations were conducted using a LC-6AD liquid chromatograph with a YMC Pack ODS-A column (250 × 20 mm, 5 μm, 120 Å) and SPD-10A VP UV/vis detector. All reagents were HPLC or analytical grade and were purchased from Tianjin Damao Chemical Company (Tianjin, People's Republic of China). Spots were detected on TLC plates under UV light or by heating after spraying with anisaldehyde/H_2SO_4 reagent.

Plant material

The fruits of *P. pubescens* L. were collected from Shenyang, Liaoning Province, China, and identified by Professor Jincai Lu, Department of Pharmaceutical Botany, School of Traditional Chinese Materia Medica, Shenyang Pharmaceutical University. A voucher specimen (CP-20110830) has been deposited in the herbarium of the Department of Natural Products Chemistry, Shenyang Pharmaceutical University.

Extraction and isolation

The fresh fruits of *P. pubescens* L. (17.5 kg) were cut into small pieces and extracted with 75% ethanol (100 L × 2). The resulting extract (1.4 kg) was concentrated in vacuo, suspended in H_2O (3 L), and partitioned successively with petroleum ether (3 L × 3), EtOAc (3 L × 3), and *n*-BuOH (3 L × 3) to give three fractions.

The EtOAc extract (66 g) was subjected to a silica gel CC (10 × 50 cm) eluted with CH_2Cl_2/MeOH (100:1, 40:1, 20:1, 10:1, 4:1, 2:1, 1:1 and 0:1 v/v) to afford nine combined fractions (E1–E9). Fraction E3 (14.0 g) was subjected to a silica gel CC (6 × 80 cm) and eluted with CH_2Cl_2/acetone (from 100:1 to 0:1, v/v) to produce eight subfractions (E31–E38). E36 (536.0 mg) was applied to a Sephadex LH-20 column (2.5 × 80 cm) eluted with CH_2Cl_2/MeOH (1:1, v/v) to give chlorophyll and E361 (380.0 mg). E361 was further separated on a silica gel CC (2.5 × 30 cm) eluted with cyclohexane/EtOAc (10:1, 5:1, 2:1, 1:1 and 0:1, v/v) to yield E3611 and E3612. Subfraction E3611 (45.0 mg) was separated by preparative

HPLC (60% MeOH/H_2O) to afford **2** (20.1 mg). Subfraction E3612 (150.0 mg) was separated by preparative HPLC (60% MeOH/H_2O) to give **1** (85.5 mg). Fraction E4 (10.5 g) was chromatographed on a silica gel column (6.0 × 80 cm) eluted with cyclohexane/EtOAc (from 100:1 to 0:1, v/v) to yield eight subfractions (E41–E48). E46 (825.0 mg) was subjected to a Sephadex LH-20 column (3.0 × 80 cm) eluted with CH_2Cl_2/MeOH (1:1, v/v) and further separated by preparative HPLC (60% MeOH/H_2O) to yield **3** (252.0 mg). Combination of E47 (2.4 g) and E48 (360.0 mg) was applied to a Sephadex LH-20 column (3.0 × 80 cm) eluted with CH_2Cl_2/MeOH (1:1, v/v) and purified using preparative HPLC (50% MeOH/H_2O) to give **5** (1.6 g) and **4** (34.0 mg).

(20*S*,22*R*,24*S*,25*S*,26*R*)-15*α*-acetoxy-5,6*β*:22,26:24,25-triepoxy-26-methoxy-4*β*-hydroxyergost-2-en-1-one (**1**). White powder (MeOH); $[\alpha]_D^{25}$: +46.9 (*c* 0.145, MeOH); UV λ_{max} (MeOH) nm (log *ε*): 213 (3.60); IR (KBr) ν_{max}: 3397, 2942, 1734, 1663, 1459, 1372, 1249, 1107, 1054 $cm^{-1;}$ ^1H NMR (300 MHz, $CDCl_3$) see Table 1; ^{13}C NMR (75 MHz, $CDCl_3$) see Table 2; HRESIMS *m/z* 567.2925 $[M+Na]^+$ (calcd. for $C_{31}H_{44}O_8Na^+$, 567.2928).

(20*S*,22*R*,24*S*,25*S*,26*R*)-15*α*-acetoxy-6*α*-chloro-22,26:24,25-diepoxy-4*β*,5*β*,26-trihydroxyergost-2-en-1-one (**2**). White powder (MeOH); $[\alpha]_D^{25}$: +50.4 (*c* 0.25, MeOH); UV λ_{max} (MeOH) nm (log *ε*): 216 (3.92); IR (KBr) ν_{max}: 3461, 2934, 1735, 1683, 1462, 1382, 1260, 1089, 1044 $cm^{-1;}$ ^1H NMR (600 MHz, $CDCl_3$) see Table 1; ^{13}C NMR (150 MHz, $CDCl_3$) see Table 2; HRESIMS *m/z* 589.2532 $[M+Na]^+$ (calcd. for $C_{30}H_{43}O_8ClNa^+$, 589.2539).

(20*S*,22*R*,24*S*,25*S*,26*S*)-15*α*-acetoxy-5,6*β*:22,26:diepoxy-24-methoxy-4*β*,25,26-trihydroxyergost-2-en-1-one (**3a**) and (20*S*,22*R*,24*S*,25*S*,26*R*)-15*α*-acetoxy-5,6*β*:22,26:diepoxy-24-methoxy-4*β*,25,26-trihydroxyergost-2-en-1-one (**3b**). White powder (MeOH); $[\alpha]_D^{25}$: −8.0 (*c* 0.345, MeOH); UV λ_{max} (MeOH) nm (log *ε*): 213 (3.80); IR (KBr) ν_{max}: 3450, 2962, 1734, 1678, 1461, 1374, 1249, 1143, 1117, 1039 $cm^{-1;}$ ^1H NMR (600 MHz, C_5D_5N) see Table 1; ^{13}C NMR (150 MHz, C_5D_5N) see Table 2; HRESIMS *m/z* 585.3033 $[M+Na]^+$ (calcd. for $C_{31}H_{46}O_9Na^+$, 585.3034).

(20*S*,22*R*,24*R*,25*S*,26*S*)-15*α*-acetoxy-5,6*β*:22,26-diepoxy-3*β*,4*β*,24,25,26-pentahydroxyergost-1-one (**4a**) and (20*S*,22*R*,24*R*,25*S*,26*R*)-15*α*-acetoxy-5,6*β*:22,26-diepoxy-3*β*,4*β*,24,25,26-pentahydroxyergost-1-one (**4b**). White powder (MeOH); $[\alpha]_D^{25}$: +73.0 (*c* 0.10, MeOH); UV end absorption; IR (KBr) ν_{max}: 3433, 2942, 1712, 1640, 1458, 1376, 1250, 1115, 1076, 1043 $cm^{-1;}$ ^1H NMR (600 MHz, C_5D_5N) see Table 1; ^{13}C NMR (150 MHz, C_5D_5N) see Table 2; HRESIMS *m/z* 584.3436 $[M+NH_4]^+$ (calcd. for $C_{30}H_{50}NO_{10}+$, 584.3435).

Molecular docking

The initial three dimensional geometric coordinates of the X-ray crystal structure of TRAIL-DR5 complex (1D4V) was downloaded from the Protein Data Bank (PDB) (http://www.pdb.org/pdb/home/home.do). Subsequently, for virtually docking analysis, Accelrys

Discovery Studio version 3.5 (Accelrys Inc., San Diego, CA, USA, 2012) with CHARMm force field parameters were used to dock the pre-generated conformations of compound **1** into TRAIL-DR5 complex. The CDOCKER protocol to the complex with CHARMm-based molecular dynamics was performed. By this way, compound **1** was allowed to be flexibly and structurally rearranged in response to the complex.

Cell lines, compounds and reagents

The human renal cell carcinoma (RCC) cell lines (786-O, A-498, Caki-2 and ACHN) and human embryonic kidney cells (HEK 293) were obtained from American Type Culture Collection (ATCC, Manassas, VA, USA). The 786-O and HEK 293 cell lines were cultured in RPMI-1640 medium supplemented with 10% fetal bovine serum (FBS); A-498 and ACHN cell lines were grown in EMEM medium supplemented with 10% FBS; Caki-2 cell line was cultured in a McCoy's medium supplemented with 10% FBS. All cells were maintained at 37 °C in a humidified atmosphere of 5% CO_2. Medium was replaced every two to three days as indicated. Pure compounds **1–5** (purity>98%) were isolated and purified by ourselves, dissolved in DMSO, aliquoted and stored at −20 °C. Antibodies for DR5, PARP, caspase-3, caspase-8, caspase-9, CHOP, Bax, and Bcl-2 were from Cell Signaling Technology (Danvers, MA, USA). Antibody for α-Tubulin was from Santa Cruz Biotechnology, Inc. (Santa Cruz, CA). Thymidine, 3-(4,5-dimethylthiazol-2-yl)-2,5-diphenyltetrazolium bromide (MTT) was obtained from Sigma (St Louis, MO, USA).

MTT assay

Briefly, cells were seeded onto 24-well plates at a density of 2×10^4 cells in 500 μL of growth medium for 24 h and then treated with compounds **1–5** at concentrations of 0, 0.15625, 0.3125, 0.625, 1.25, 2.5, 5 and 10 μM for 72 h, respectively. In addition, 786-O cells were treated with different concentrations of **1** (0, 1, 2 μM) with or without TRAIL (0, 50, 100 ng/mL) added to each well to study the combined effects of **1** and TRAIL. After 72 h incubation, 200 μL of MTT solution was added to each well and incubated at 37 °C for 2 h. HEK 293 cells were treated with different concentrations of **1** (0, 1.25, 2.5, 5, 10 μM) for 48 or 72 h, then 200 μL of MTT solution was added to each well and incubated at 37 °C for 2 h. The MTT solution was then aspirated and 200 μL of dissolving buffer was added to each well. Cell viability was determined by measuring absorbance at 570 nm in a microplate reader (Bio-Rad, Hercules, CA, USA). Dose response curves were then generated as a percentage of vehicle control treated cells using Excel software, and IC_{50} values were determined graphically from the plot.

DAPI nuclear staining

786-O cells (4×10^4 cells/well) were cultured on chamber slides for 24 h. Then, the cells were treated with different concentrations of compound **1** for 24 h. After treatment, cells were then rinsed in 1 × PBS for 3 times, and fixed in 4% paraformaldehyde. Fixed cells were mounted in Vector shield medium containing DAPI (Vector Laboratories, Inc., Burlingame, CA) in a dark place and visualized with a Nikon Eclipse TE2000-S (200 × magnification) microscope under ultraviolet light. Apoptotic cells were identified by the nuclear condensation and fragmentation.

Protein isolation and Western blot analysis

Cells were treated with compound **1** at varying concentrations for 24 h, and protein lysates were then prepared in RIPA lysis buffer containing protease inhibitors (Sigma, St Louis, MO, USA). Volumes of clarified protein lysate containing equal amounts of protein (50 μg) were separated on 10–12% sodium dodecyl sulfate-polyacrylamide gel electrophoresis (SDS-PAGE) and electrophoretically (90 min at 100 V) transferred to a Hybond-ECL membrane (GE Healthcare, Piscataway, NJ, USA). Blots were then blocked for 1 h in 1 × TBST (10 mM Tris-HCl, pH 8.0, 150 mM NaCl, and 0.05% Tween-20) containing 5% blocking grade non-fat dry milk (Bio-Rad, Hercules, CA, USA), and then incubated overnight with primary antibody at 4 °C. Blots were then washed for three times in 1 × TBST and incubated for 2 h at room temperature with HRP-conjugated goat anti-rabbit or anti-mouse IgG secondary antibody (Santa Cruz Biotechnology, Santa Cruz, CA, USA). Immunoreactive bands were visualized using an enhanced chemiluminescence detection system (Thermo Scientific, Rockford, IL, USA).

Caspase activity assay

The Caspase-Glo® 3/7 and Caspase-Glo® 8 Assays (Promega, Madison, WI) for measuring caspase-3/7 and caspase-8 activities in treated cells, respectively, were performed according to the manufacturer's instructions. Briefly, 786-O cells were cultured on a 24-well plate and treated with 0.1% DMSO (vehicle control) or **1** (0.5, 1 and 2 μmol/L) for 24 h. Then 100 μL of Caspase-Glo® 3/7 or Caspase-Glo® 8 reagent was added into each well and the luminescence of each sample was measured in a luminometer (GloMax®-MultiDetection System).

Flowcytometric analysis of apoptosis

786-O cells were seeded at a density of 4×10^5 per dish (10 cm) and incubated for 24 h. Then, the cells were treated with compound **1** at indicated concentrations for 24 or 72 h. The cells were harvested and rinsed with 1 × PBS. The collected cells were fixed with 500 μL of 1 × PBS and 10 mL of 70% ethanol at 4 °C for 18 h; then after washing twice with 1 × PBS, they were stained with fluorescein (FITC-conjugated Annexin V and propidium iodide in PBS according to the manufacturer's protocol (PharMingen)). The analyses of cells were done by using appropriate scatter gates to exclude cellular aggregated and debris cells. Ten thousand events were collected for each sample.

Rhodamine 123 staining and measurement of mitochondrial membrane potential (MMP)

Mitochondrial membrane potential was measured by a membrane-permeable cationic fluorescent dye (Rhodamine 123). After incubation with compound **1** for indicated time, the cells were incubated with Rhodamine 123 in the dark at 37 °C for 30 min, then the morphology was observed by a fluorescence microscopy (Olympus, Tokyo, Japan). To measure the mitochondrial membrane potential (MMP), cells were stained with Rhodamine 123, then harvested and suspended in 400 μL 1 × PBS. The samples were subsequently analyzed by a FACScan flow cytometry (Becton Dickinson, Franklin Lakes, NJ).

Supplementary Material

Refer to Web version on PubMed Central for supplementary material.

Acknowledgments

This work was financially supported by grants from the National Natural Science Foundation of China (NSFC) (31270399 and 21472138), Key Projects of the National Science and Technology Pillar Program (2012BAI30B02), the Project of Innovation Team (LT2015027) of Liaoning of P. R. China, Fund of the Educational Department of Liaoning Province (L2011177), Liaoning Baiqianwan Talents Program (2013921043), Scientific Research Foundation for the Returned Overseas Chinese Scholars of Shenyang Pharmaceutical University (GGJJ2015103) and 2015 Career Development Program for Young and Middle-aged Teachers of Shenyang Pharmaceutical University.

This work was also in part supported by NIH awards 5R01CA122558-05 and 1R21CA152804-01A1 (to X. Zi).

Notes and references

1. Jonasch E, Gao J, Rathmell WK. Br Med J. 2014; 349:g4797. [PubMed: 25385470]
2. Siegel R, Ma J, Zou Z, Jemal A. CA Cancer J Clin. 2014; 64:9–29. [PubMed: 24399786]
3. Pennarun B, Meijer A, de Vries EG, Kleibeuker JH, Kruyt F, de Jong S. Biochim Biophys Acta. 2010; 1805:123–140. [PubMed: 19961901]
4. Micheau O, Shirley S, Dufour F. Br J Pharmacol. 2013; 169:1723–1744. [PubMed: 23638798]
5. Pan G, Ni J, Wei YF, Yu G, Gentz R, Dixit VM. Science. 1997; 277:815–818. [PubMed: 9242610]
6. Stolfi C, Pallone F, Monteleone G. Int J Mol Sci. 2012; 13:7886–7901. [PubMed: 22942679]
7. Ndozangue-Touriguine O, Sebbagh M, Mérino D, Micheau O, Bertoglio J, Bréard J. Oncogene. 2008; 27:6012–6022. [PubMed: 18560353]
8. Liu Y, Yang ZY, Gong C, Zhang LY, Yu GL, Gong W. Cancer Sci. 2014; 105:520–527. [PubMed: 24612139]
9. Yadav VR, Prasad S, Aggarwal BB. Br J Pharmacol. 2012; 165:741–753. [PubMed: 21797841]
10. Tang Y, Li X, Liu Z, Simoneau AR, Xie J, Zi X. Int J Cancer. 2010; 127:1758–1768. [PubMed: 20112340]
11. Misico RI, Nicotra VE, Oberti JC, Barboza G, Gil RR, Burton G. Prog Chem Org Nat Prod. 2011; 94:127–229. [PubMed: 21833839]
12. Chen LX, HH, Qiu F. Nat Prod Rep. 2011; 28:705–740. [PubMed: 21344104]
13. Kithsiri WEM, Xu YM, Scherz-Shouval R, Marron MT, Rocha DD, Liu MX, Costa-Lotufo LV, Santagata S, Lindquist S, Whitesell L, Gunatilaka AAL. J Med Chem. 2014; 57:2851–2863. [PubMed: 24625088]
14. Zhang HP, Samadi AK, Gallagher RJ, Araya JJ, Tong XQ, Day VW, Cohen MS, Kindscher K, Gollapudi R, Timmermann BN. J Nat Prod. 2011; 74:2532–2544. [PubMed: 22098611]
15. Yang BY, Guo R, Li T, Wu JJ, Zhang J, Liu Y, Wang QH, Kuang HX. Steroids. 2014; 87:26–34. [PubMed: 24844203]
16. Qiu L, Zhao F, Jiang ZH, Chen LX, Zhao Q, Liu HX, Yao XS, Qiu F. J Nat Prod. 2008; 71:642–646. [PubMed: 18348534]
17. Yang BY, Xia YG, Liu Y, Li L, Jiang H, Yang L, Wang QH, Kuang HX. Phytochem Lett. 2014; 8:92–96.
18. Kour K, Pandey A, Suri KA, Satti NK, Gupta KK, Bani S. Int Immunopharmacol. 2009; 9:1137–1144. [PubMed: 19524704]
19. Zhang WN, Tong WY. Chem Biodiversity. 2016; 13:48–65.
20. Xu L, Wang RX, Yang YY, Wang B. Zhongguoyeshengzhiwuziyuan. 2009; 28:21–23.
21. Glotter E, Sahai M, Kirson I. J Chem Soc Perkin Trans I. 1985:2241–2245.
22. Ji L, Yuan YL, Ma ZJ, Chen Z, Gan LS, Ma XQ, Huang DS. Steroids. 2013; 78:860–865. [PubMed: 23685089]

23. Kirson I, Glotter E, Lavie D, Abraham A. J Chem Res. 1980; 4:2134–2156.
24. Nicotra VE, Basso AV, Ramacciotti NS, Misico RI. J Nat Prod. 2013; 76:2219–2225. [PubMed: 24303781]
25. Chao CH, Chou KJ, Wen ZH, Wang GH, Wu YC, Dai CF, Sheu JH. J Nat Prod. 2011; 74:1132–1141. [PubMed: 21425785]
26. Nittala SS, Velde VV, Frolow F, Lavie D. Phytochemistry. 1981; 20:2547–2552.
27. Bonetto GM, Gil RR, Oberti JC, Veleiro AS, Burton G. J Nat Prod. 1995; 58:705–711.
28. Pelletier SW, Gebeyehu G, Nowacki J, Mody NV. Heterocycles. 1981; 15:317–320.
29. Chen BW, Chen YY, Lin YC, Huang CY, Uvarani C, Hwang TL, Chiang MY, Liug HY, Sheu JH. RSC Adv. 2015; 5:88841–88847.
30. Zi X, Simoneau AR. Cancer Res. 2005; 65:3479–3486. [PubMed: 15833884]
31. Finnberg N, El-Deiry WS. Cell Cycle. 2008; 7:1525–1528. [PubMed: 18469516]
32. Martinou JC, Green DR. Nat Rev Mol Cell Biol. 2001; 2:63–67. [PubMed: 11413467]
33. Wang X. Genes Dev. 2001; 15:2922–2933. [PubMed: 11711427]
34. Yoshida T, Shiraishi T, Nakata S, Horinaka M, Wakada M, Mizutani Y, Miki T, Sakai T. Cancer Res. 2005; 65:5662–5667. [PubMed: 15994939]
35. Henrich CJ, Brooks AD, Erickson KL, Thomas CL, Bokesch HR, Tewary P, Thompson CR, Pompei RJ, Gustafson KR, McMahon JB, Sayers TJ. Cell Death Dis. 2015; 6:e1666. [PubMed: 25719250]
36. Lee TJ, Um HJ, Min DS, Park JW, Choi KS, Kwon TK. Free Radic Biol Med. 2009; 46:1639–1649. [PubMed: 19345731]
37. Damu AG, Kuo PC, Su CR, Kuo TH, Chen TH, Bastow KF, Lee KH, Wu TS. J Nat Prod. 2007; 70:1146–1152. [PubMed: 17580910]
38. Llanos GG, Araujo LM, Jiménez IA, Moujir LM, Vázquez JT, Bazzocchi IL. Steroids. 2010; 75:974–978. [PubMed: 20542049]
39. Machin RP, Veleiro AS, Nicotra VE, Oberti JC, Padròn JM. J Nat Prod. 2010; 73:966–968. [PubMed: 20438092]
40. Zhang HP, Samadi AK, Gallagher RJ, Araya JJ, Tong XQ, Day VW, Cohen MS, Kindscher K, Gollapudi R, Timmermann BN. J Nat Prod. 2011; 74:2532–2544. [PubMed: 22098611]

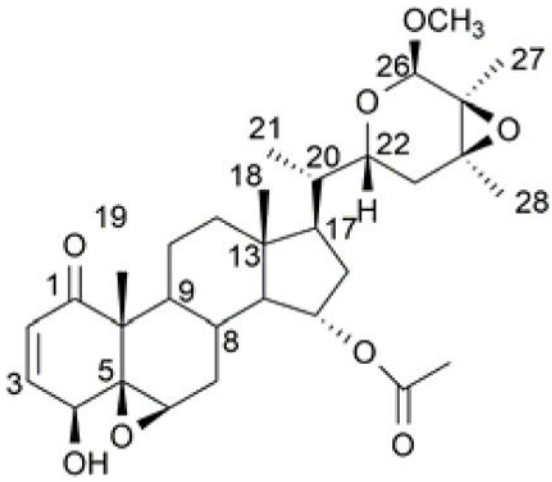

1

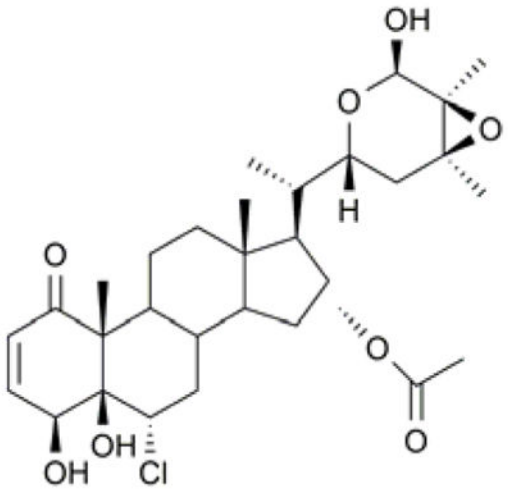

2

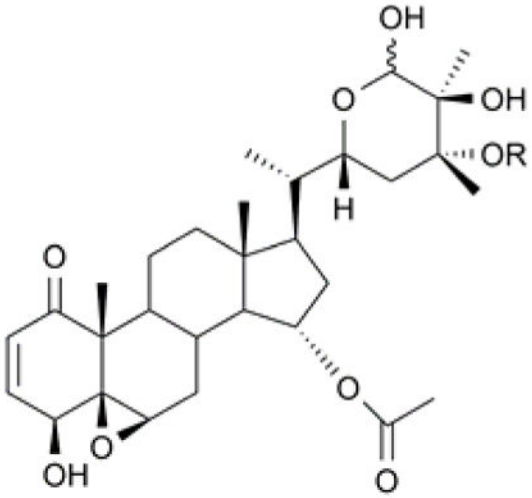

3a R=CH_3 (26α -OH)
3b R=CH_3 (26β -OH)
5a R=H (26α -OH)
5b R=H (26β -OH)

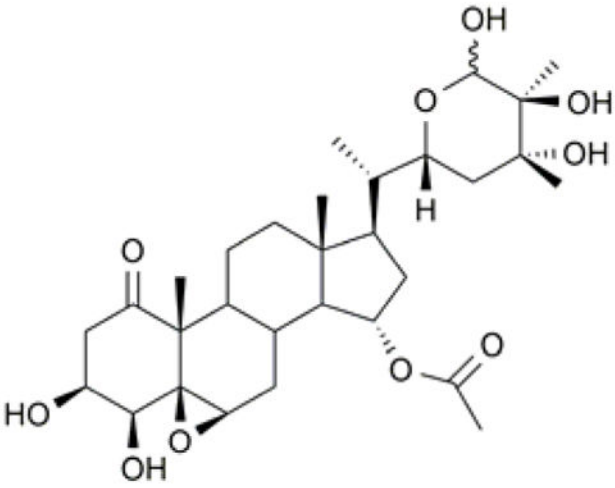

4a 26α -OH
4b 26β -OH

Figure 1.
Structures of compounds **1**–**5**.

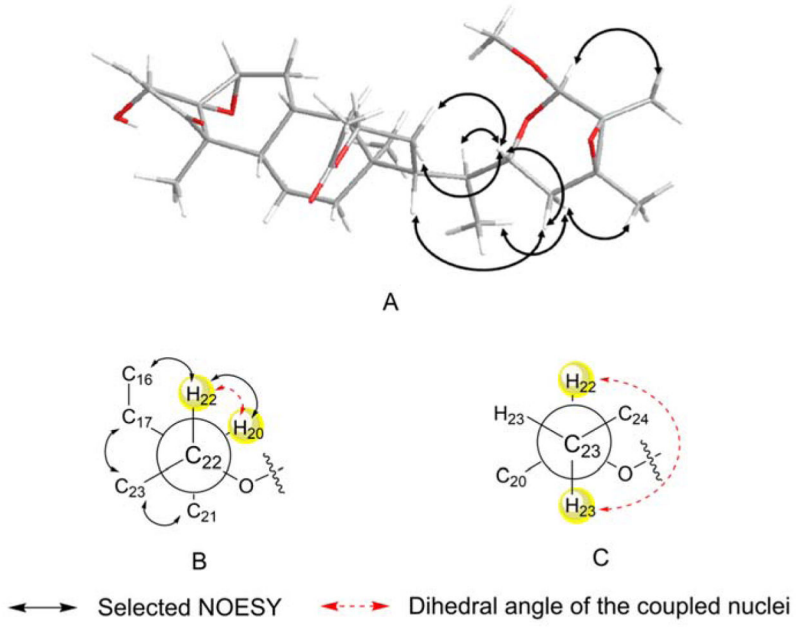

Figure 2.

Selected NOESY correlations (A) and Newman projections for C-22/C-20 rotamer (B) and C-23/C-22 rotamer (C) of compound **1.**

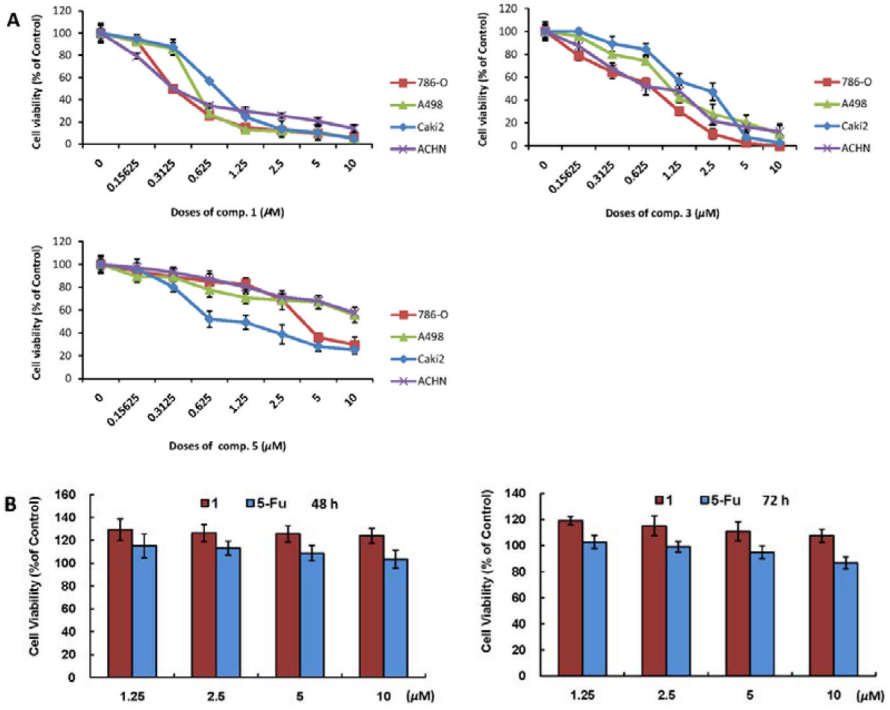

Figure 3.

The inhibitory effects of compounds **1**, **3** and **5** on the growth of human RCC cell lines (786-O, A498, Caki-2 and ACHN) and cytotoxicity of **1** on human embryonic kidney cells (HEK 293). (A) Cells in 24-well culture plates were treated with vehicle control (0.1% DMSO), and **1**, **3** and **5** at the indicated concentrations. After 72 h of treatment, cell viabilities were measured by MTT assay. Each point is the mean of values from three independent plates; bars, SD. IC_{50}s were estimated by dose-response curves. (B) The cytotoxicity of **1** in normal human cells (human embryonic kidney cells, HEK 293) compared with 5-fluorouracil (5-Fu) was measured using an MTT assay. The HEK 293 cells were treated with **1** and 5-Fu at 1.25–10 μM for 48 and 72 h. Each point is the mean of values from three independent plates; bars, SD.

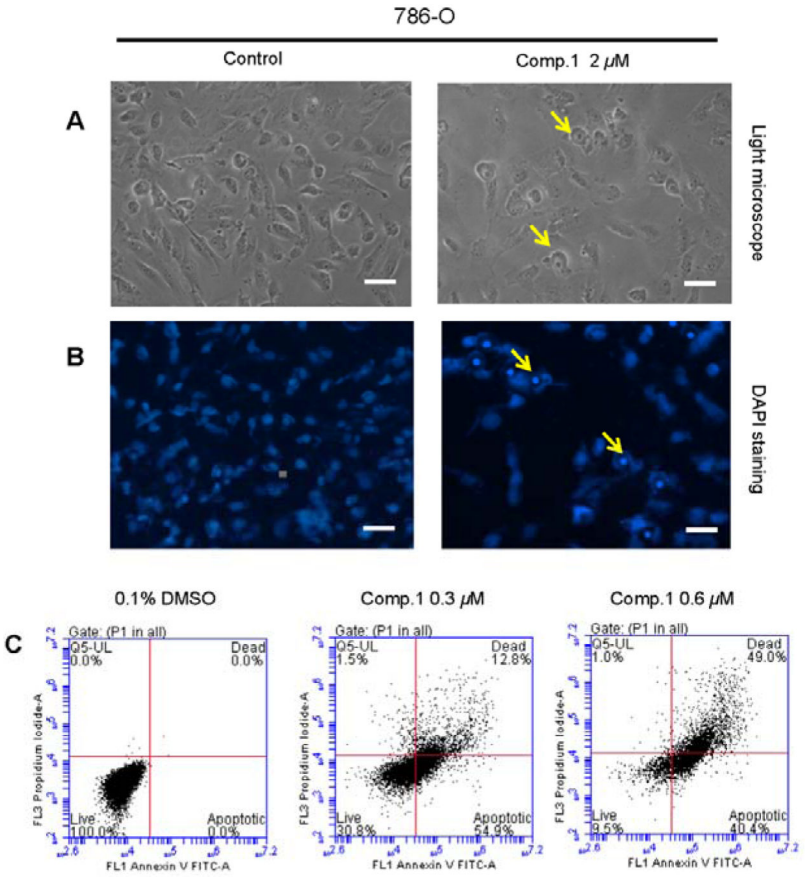

Figure 4.

Compound **1** induces apoptosis in 786-O cells. (A) RCC cell morphology under phase-contrast light microscope (Magnification: × 200, bar = 20 μm). A representative picture was shown from a random field. (B) DAPI staining of nuclear morphology under fluorescence microscope (Magnification: × 200, bar = 20 μm). A representative picture was shown from a random field. (C) The cells were treated with 0.3 and 0.6 μM **1** for 72 h. After stained by AnnexinV and PI, the cells were analyzed by flowcytometry. Data represent the means from 3 independent experiments. Standard errors are less than 5%.

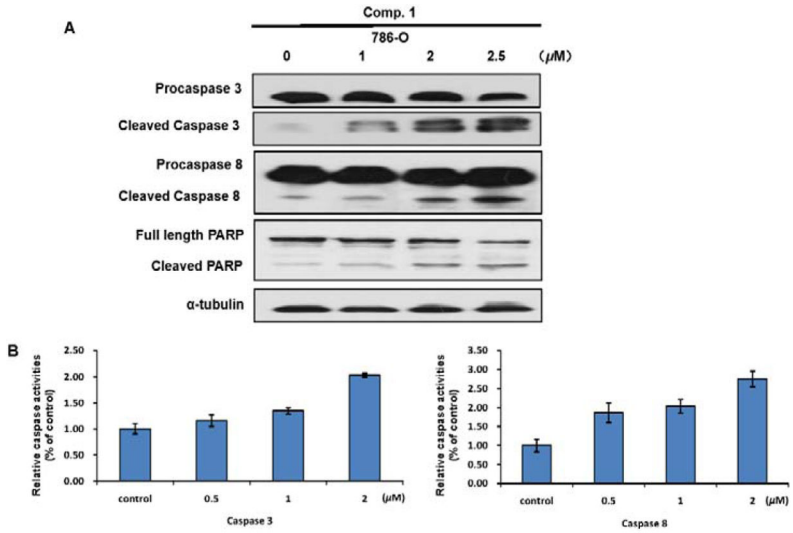

Figure 5.

The apoptosis induced by compound **1** depends on caspase-3 and caspase-8. (A) 786-O Cells were treated with 1, 2, 2.5 μM **1** for 24 h. Cleavage of caspase-3, caspase-8, and PARP was detected by Western blot analysis. α-Tubulin was used as a loading control. A representative blot was shown from three independent experiments. (B) 786-O Cells were treated with 0.5, 1, 2 μM **1** for 24 h. Caspase activation was determined with caspase-3/7 and caspase-8 activity assays.

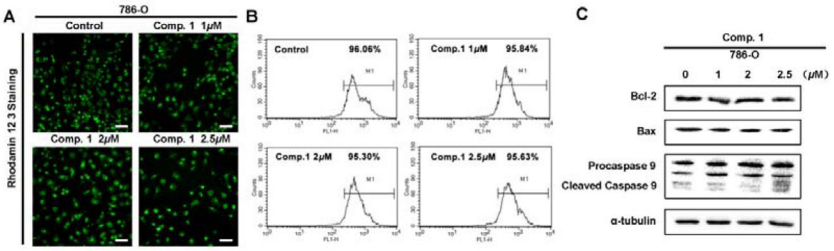

Figure 6.

The apoptosis induced by compound **1** is not correlated with caspase-9. (A and B) 786-O Cells were cultured in the presence of 1, 2, 2.5 μM **1** for 24 h, then incubated with Rhodamine 123 in the dark at 37 °C for 30 min, then the morphology was observed by a fluorescence microscopy (Magnification: × 200, bar = 50 μm) (A), and the mitochondrial membrane potential ($\Delta\psi$m) was measured by flow cytometric analysis (B). A representative picture was shown from a random field. (C) 786-O Cells were treated with 1, 2, 2.5 μM **1** for 24 h. The protein levels of Bcl-2, Bax, and caspase-9 were detected by Western blot analysis. α-Tubulin was used as a loading control. A representative blot was shown from three independent experiments.

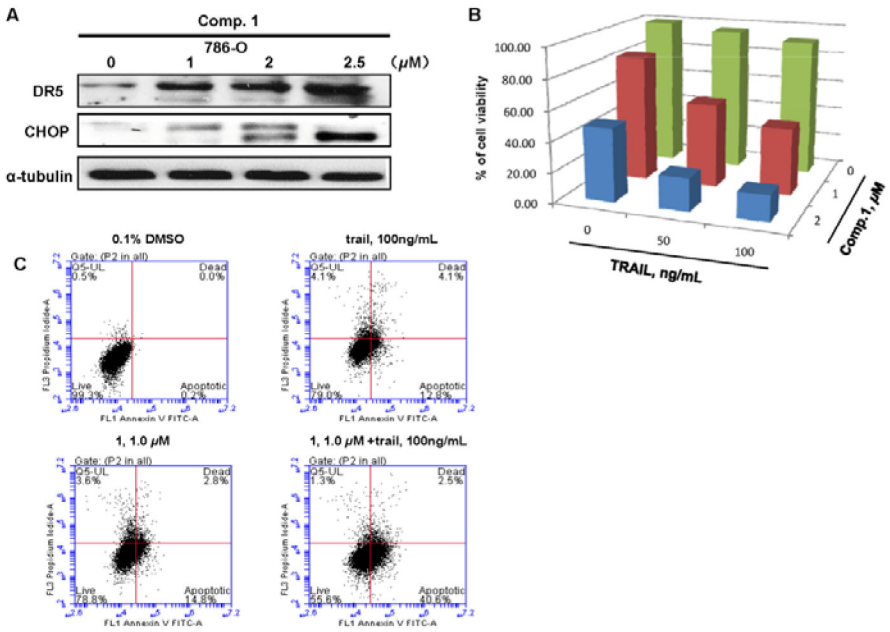

Figure 7.

Compound **1** effects on TRAIL sensitization in 786-O cells. (A) 786-O Cells were treated with 1, 2, 2.5 μM **1** for 24 h. Protein levels of DR5 and CHOP were detected by Western blot analysis. α-Tubulin was used as a loading control. A representative blot was shown from three independent experiments. (B) The combined effect of **1** (0, 1, 2 μM) and TRAIL (0, 50, 100 ng/mL) on 786-O cell viability. Columns, mean for percentage of cell viability relative to control (n=3). (C) The combined effect of **1** (1 μM) and TRAIL (100 ng/mL) on apoptosis of 786-O cells. The cells were treated with 1 μM **1** for 24 h, and were stained by Annexin V and PI and analyzed by flowcytometry. Data represent the means from 3 independent experiments. Standard errors are less than 5%.

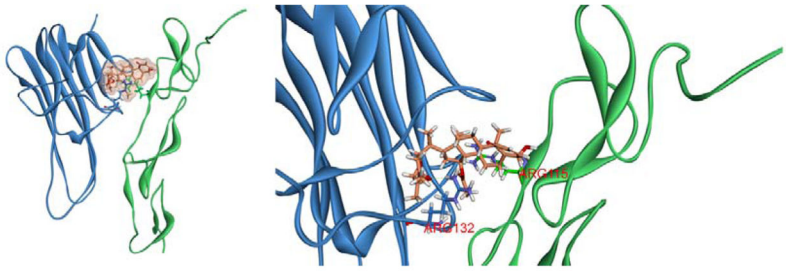

Figure 8.

(A) Docked conformation of compound **1** with TRAIL-DR5 complex. (B) Binding modes of compound **1** with the key residues of TRAIL-DR5 complex.

RSC Adv. Author manuscript; available in PMC 2017 May 26.

Table 1

^{1}H NMR Spectroscopic Data of Compounds **1, 2, 3a/3b** and **4a/4b**[a], δ in ppm

	1	**2**	**3a***	**3b***	**4a***	**4b***
position	**δ_H, (J in Hz)**	**δ_H, (J in Hz)**	**δ_H, (J in Hz)**	**δ_H, (J in Hz)**	**δ_H, (J in Hz)**	**δ_H, (J in Hz)**
2	6.16, d (10.0)	6.00, d (10.2)	6.47, d (9.8)	6.47, d (9.8)	3.41, dd (15.4,7.7)	3.41, dd (15.4,7.7)
					3.21, dd (15.4,3.5)	3.21, dd (15.4,3.5)
3	6.90, dd (10.0, 5.8)	6.47, dd (10.2, 1.5)	7.28, dd (9.8, 6.2)	7.28, dd (9.8, 6.2)	4.74, m	4.74, m
4	3.72, d (5.8)	5.05, br s	4.04, d (6.2)	4.04, d (6.2)	4.01, br s	4.01, br s
6	3.19, br s	4.37, dd (11.8, 4.3)	3.20, br s	3.20, br s	3.68, br s	3.68, br s
7	2.04, dd (15.1, 4.1)	2.20, m	2.20, dd (15.1, 4.1)	2.20, dd (15.1, 4.1)	2.38, br d (15.4)	2.38, br d (15.4)
	1.43, m	1.78, m	1.51, m	1.51, m	1.88, m	1.88, m
8	1.67, m	1.79, m	1.82, m	1.82, m	1.80, m	1.80, m
9	1.05, td (11.5, 4.1)	1.31, td (11.6, 4.1)	1.11, td (11.5, 4.1)	1.11, td (11.5, 4.1)	1.61, td (12.1, 4.2)	1.61, td (12.1, 4.2)
11	1.82, m	1.31, m	2.00, m	2.00, m	1.57, m	1.57, m
	1.42, m	0.90, m	1.52, m	1.52, m	1.50, m	1.50, m
12	1.89, dt (12.5, 3.5)	1.86, dt (12.5, 3.5)	1.87, dt (12.6, 3.2)	1.87, dt (12.6, 3.2)	1.83, dt (12.9, 3.8)	1.83, dt (12.9, 3.8)
	1.18, m	1.11, m	1.13, m	1.13, m	1.10, td (12.9, 3.7)	1.10, td (12.9, 3.7)
14	1.22, m	1.34, m	1.34, m	1.34, m	1.34, t (10.0)	1.34, t (10.0)
15	4.80, td (9.5, 3.2)	4.81, td (9.6, 2.8)	4.98, td (9.5, 2.8)	4.98, td (9.5, 2.8)	5.00, td (9.5, 3.1)	5.00, td (9.5, 3.1)
16	2.01, m	2.09, m	2.18, m	2.18, m	2.13, m	2.13, m
	1.53, m	1.52, m	1.75, m	1.75, m	1.78, m	1.78, m
17	1.26, m	1.29, m	1.47, m	1.47, m	1.46, m	1.46, m
18	0.72, s	0.69, s	0.61, s	0.59, s	0.61, s	0.59, s
19	1.38, s	1.23, s	1.85, s	1.85, s	1.78, s	1.77, s
20	1.60, m	1.66, m	1.97, m	1.97, m	1.99, m	1.92, m
21	0.86, d (6.7)	0.82, d (6.6)	1.10, d (6.4)	1.10, d (6.4)	1.12, d (6.4)	1.11, d (6.4)
22	3.67, dt (10.0, 3.6)	3.57, dt (9.3, 3.7)	3.73, dt (12.4, 2.9)	4.41, dt (12.4, 2.8)	3.82, dt (12.4, 2.5)	4.49, dt (12.4, 2.5)
23	1.67, m	1.62, m	1.86, m	2.23, m	2.18, m	2.25, m
	1.58, m	1.58, m	1.62, m	1.85, m	1.74, m	1.86, m
26	4.58, s	4.95, s	5.25, s	5.36, s	5.39, s	5.52, s
27	1.33, s	1.38, s	1.82, s	1.67, s	1.96, s	1.81, s

	1	2	3a*	3b*	4a*	4b*
position	**δ_H, (*J* in Hz)**	**δ_H, (*J* in Hz)**	**δ_H, (*J* in Hz)**	**δ_H, (*J* in Hz)**	**δ_H, (*J* in Hz)**	**δ_H, (*J* in Hz)**
28	1.33, s	1.37, s	1.56, s	1.79, s	1.77, s	1.99, s
AcO-15	1.98, s	2.03, s	2.09, s	2.08, s	2.04, s	2.03, s
MeO-24			3.56, s	3.55, s		
MeO-26	3.37, s					

[a]Spectrum of compound **1** was measured at 300 MHz, spectra of compounds **2, 3a/3b** and **4a/4b** were measured at 600 MHz; spectra of **1** and **2** were obtained in $CDCl_3$ spectra of **3a/3b** and **4a/4b** were obtained in C_5D_5N.

*3a and 4a correspond to the 26*S* epimers; **3b** and **4b** correspond to the 26*R* epimers.

Table 2

^{13}C NMR Spectroscopic Data of Compounds**1, 2, 3a/3b** and **4a/4b**[a], δ in ppm

	1	**2**	**3a***	**3b***	**4a***	**4b***
position	**δ_C, type**	**δ_C, type**	**δ_C, type**	**δ_C, type**	**δ_C, type**	**δ_C, type**
1	202.3, C	199.9, C	202.9, C	202.9, C	210.9, C	210.9, C
2	132.1, CH	127.7, CH	132.7, CH	132.7, CH	44.4, CH_2	44.4, CH_2
3	142.1, CH	142.9, CH	145.6, CH	145.6, CH	69.6, CH	69.6, CH
4	69.8, CH	66.1, CH	70.7, CH	70.7, CH	79.1, CH	79.1, CH
5	63.6, C	77.9, C	64.7, C	64.7, C	65.5, C	65.5, C
6	62.6, CH	66.4, CH	60.5, CH	60.5, CH	59.3, CH	59.3, CH
7	30.4, CH_2	38.8, CH_2	31.4, CH_2	31.4, CH_2	31.7, CH_2	31.7, CH_2
8	29.2, CH	34.3, CH	30.1, CH	30.1, CH	30.0, CH	30.0, CH
9	43.8, CH	45.7, CH	44.5, CH	44.5, CH	43.2, CH	43.2, CH
10	47.6, C	57.0, C	48.7, C	48.7, C	51.3, C	51.3, C
11	22.2, CH_2	22.6, CH_2	22.0, CH_2	22.0, CH_2	22.0, CH_2	22.0, CH_2
12	39.5, CH_2	39.2, CH_2	39.9, CH_2	39.9, CH_2	39.7, CH_2	39.7, CH_2
13	43.0, C	43.4, C	43.5, C	43.5, C	43.5, C	43.5, C
14	58.9, CH	58.3, CH	59.3, CH	59.4, CH	59.1, CH	59.2, CH
15	75.9, CH	75.4, CH	76.1, CH	76.4, CH	76.6, CH	76.5, CH
16	37.7, CH_2	36.9, CH_2	37.7, CH_2	37.9, CH_2	37.7, CH_2	37.8, CH_2
17	50.1, CH	50.3, CH	50.7, CH	51.4, CH	51.1, CH	51.4, CH
18	12.7, CH_3	12.9, CH_3	13.1, CH_3	13.0, CH_3	13.1, CH_3	13.0, CH_3
19	17.6, CH_3	9.9, CH_3	17.6, CH_3	17.6, CH_3	16.0, CH_3	16.0, CH_3
20	38.9, CH	38.6, CH	39.8, CH	39.6, CH	39.7, CH	39.5, CH
21	12.9, CH_3	12.6, CH_3	13.7, CH_3	13.7, CH_3	13.8, CH_3	13.7, CH_3
22	65.9, CH	64.7, CH	73.0, CH	68.6, CH	73.2, CH	69.1, CH
23	30.2, CH_2	29.5, CH_2	35.7, CH_2	35.8, CH_2	37.5, CH_2	37.8, CH_2
24	61.3, C	64.9, C	78.6, C	77.6, C	77.6, C	75.7, C
25	61.1, C	63.9, C	77.9, C	76.5, C	74.3, C	73.2, C
26	99.3, CH	91.7, CH	98.3, CH	99.5, CH	98.6, CH	99.4, CH

	1	2	3a*	3b*	4a*	4b*
position	**δ_C, type**	**δ_C, type**	**δ_C, type**	**δ_C, type**	**δ_C, type**	**δ_C, type**
27	17.1, CH_3	16.6, CH_3	16.2, CH_3	22.6, CH_3	16.3, CH_3	22.8, CH_3
28	18.7, CH_3	19.0, CH_3	17.5, CH_3	19.2, CH_3	23.8, CH_3	25.7, CH_3
AcO-15	170.5, C	170.7, C	171.0, C	170.9, C	171.0, C	170.9, C
	21.4, CH_3	21.4, CH_3	21.7, CH_3	21.7, CH_3	21.7, CH_3	21.7, CH_3
MeO-24			50.9, CH_3	50.7, CH_3		
MeO-26	55.7, CH_3					

[a]Spectrum of compound **1** was measured at 75 MHz, spectra of compounds **2, 3a/3b** and **4a/4b** were measured at 150 MHz; spectra of **1** and **2** were obtained in $CDCl_3$, spectra of **3a/3b** and **4a/4b** were obtained in C_5D_5N.

*__3a__ and __4a__ correspond to the 26*S* epimers; __3b__ and __4b__ correspond to the 26*R* epimers.

RSC Adv. Author manuscript; available in PMC 2017 May 26.